Korean J. Chem. Eng., **25**(4), 825-832 (2008)

Water adsorption in activated carbons with different burn-offs and its analysis using a cluster model

Supunnee Junpirom*, Chaiyot Tangsathitkulchai*,†, Malee Tangsathitkulchai, and Yuvarat Ngernyen***

*School of Chemical Engineering, Institute of Engineering, Suranaree University of Technology, Nakhon Ratchasima 30000, Thailand
**School of Chemistry, Institute of Science, Suranaree University of Technology, Nakhon Ratchasima 30000, Thailand
(*Received 11 January 2007 • accepted 11 December 2007*)

Abstract−This work presents the behavior of water adsorption in the activated carbons with different porous structure derived by varying the level of char burn-off. Water adsorption isotherms of activated carbons prepared from longan seed at three different burn-offs (19, 26 and 60%) were measured gravimetrically. These obtained carbons were different in terms of their pore size distribution and also the surface functional group properties by showing an increasing of total pore volume and the concentration of surface functional groups with increasing in the burn-off level. The water adsorption isotherms showed that the behavior and amount of water uptake could be divided into three consecutive ranges of relative pressure, 0.0-0.3, 0.3-0.7 and 0.7-0.94, corresponding to adsorption in ultramicropores, supermicropores, and mesopores, respectively. The isotherm data were simulated by a cluster model proposed by Do and Do. The correlation was found to be satisfactory over the entire range of relative pressure only with the lowest burn-off carbon which contained mainly micropores. For higher burn-off carbons, which showed increasing proportions of mesopores, the model needed to be modified by increasing the cluster size of the adsorbed water molecules from 5 to 20 for adsorption at relative pressures greater than about 0.7.

Key words: Activated Carbon, Activation, Longan Seed, Water Adsorption, Cluster Models

INTRODUCTION

Adsorption by employing activated carbon as an adsorbent is widely applied in numerous industrial processes of separation and purification. Activated carbon, which has high adsorptive capacity due to its large surface area and pore volume, is capable of adsorbing a variety of substances from both liquid and gaseous systems [1,2]. The presence of chemically inert graphite surface area renders the activated carbon surface to be non-polar in nature [Kim et al., 2003]. However, it can also adsorb several different polar molecules such as water with a significant adsorption capacity. This behavior sometimes creates a problem in practical adsorption processes, such as in the process of VOC removal from air since water is always present in air. Furthermore, it is also known that the efficiency of many industrial adsorbers can be largely affected even by the quite low humidity of the entering gases [4-6]. However, to date the mechanism of water vapor adsorption on porous solid is not fully understood.

Water adsorption behavior on activated carbon is quite different from that of the other simple fluids such as nitrogen, carbon dioxide or hydrocarbons. There has been considerable research effort to better understand water adsorption behavior, including conducting experimental investigation, proposing isotherm equation models as well as molecular simulation study. Foley et al. [4] studied the kinetics of water vapor adsorption on coconut shell activated carbon. They found that the rate of adsorption and desorption depended on the relative pressure of isotherm and the slowest rate occurred in the region of relative humidity in the range 40-70%. Water adsorption experiments on a series of oxidized wood and coal based-activated carbons were conducted by Salame and Bandosz [7]. Their results showed that the isosteric heat of water adsorption was affected by surface chemical heterogeneity only at low surface coverage and the limiting heat of adsorption was equal to the heat of water condensation of 45 kJ/mol. The water adsorption mechanism was also proposed by many research groups. The most plausible theory is the one proposed by Dubinin and Serpinsky (DS equation) [8]. Based on this DS theory, water molecules first adsorb at the oxygenated groups on the carbon surface. Then, these pre-adsorbed sites further act as the primary adsorption centers for more molecules to adsorb on. This model equation enabled some experimental data to be described, but it failed to explain the adsorption isotherms in some cases, especially for carbons with a large number of surface functional groups [5].

Do and Do [5] proposed a model which is more general in dealing with the different shapes of water isotherms for carbonaceous materials. The model assumptions were based on the growth of water clusters around the surface functional groups at the edges of the basal planes of the graphitic units by forming a pentamer cluster with subsequent adsorption of these clusters into the micropores. Furthermore, molecular simulations have also been used to investigate the phenomenon of water adsorption on activated carbons. Müller et al. [9,10] and McCallum et al. [11] used the grand canonical Monte Carlo simulation to find that the adsorption of water occurs via the formation of three-dimensional clusters on surface active sites. The adsorption also depended strongly on the density and the strength of oxygen surface groups. Recently, Birkett and Do [12] reported that water adsorption behavior was strongly influenced by both the pore width and the surface functional groups as found in their simulation study of water adsorption in finite carbon pores. Study on the

†To whom correspondence should be addressed.
E-mail: chaiyot@sut.ac.th

role of surface functional groups on water adsorption by using the oxidation treatment or modification of the carbon surface has also been reported [7]. This work produced carbon with surface chemistry different from the original one. As a result of surface modification, the water adsorption mechanism is influenced more by the role of surface functional group than by the effect of pore size distribution alone. However, Kaneko and coworkers [13] suggested that water can also be adsorbed via clusterization on hydrophobic carbon nanopore surface free of surface functional groups. The stabilization resulting from cluster developing reduces the hydrophilicity of water molecules, giving a less hydrophilic cluster that can be attracted to the hydrophobic surface of carbon [14,15].

This work was aimed primarily at investigating the water adsorption behavior on activated carbons with different porous structure prepared by varying the level of char burn-off. This controlled change of char burn-off not only affects the pore size distribution of the carbons but probably the types, concentration and distribution of surface functional groups as well. However, no attempt was made at this stage to conduct detailed investigation as to the role of surface functional groups on water adsorption by altering the surface chemistry of carbon with some oxidizing agents. In this study, a series of activated carbon was produced from longan seed by carbon dioxide activation. In addition, a commercial coconut shell based activated carbon was also studied for the purpose of comparison. Isotherm measurements were carried out by using a gravimetric adsorption technique. Due to the model simplicity and the ability to describe various water isotherms, the model proposed by Do and Do [5] was adopted to simulate the water adsorption isotherms in the present study.

MATERIALS AND METHODS

1. Preparation and Characterization of Activated Carbons

Activated carbons prepared from longan seed at three different char burn-offs and a commercial activated carbon were used in this study. The longan seed, which is the inner part of longan fruit, is an abundant solid waste produced from the fruit cannery in Thailand. This waste is considered as a potential precursor for activated carbon production. Preparation of longan seed activated carbons was as follows. The pre-dried longan seed was crushed and sieved to obtain a sample fraction with the average screen size of 2.1 mm (8× 10 mesh) and then carbonized in a horizontal tube furnace (Carbolite, UK) at 650 °C for 2 h under a constant flow of nitrogen (100 cc/min), giving a char with 30 percent yield. Next, the char was activated in the same tube furnace under a constant flow of carbon dioxide (100 cc/min) at different holding times and temperatures to obtain activated carbons with different degrees of char burn-off. The three burn-off series of 19, 26 and 60% were chosen for adsorption study and referred to as LAC1, LAC2 and LAC3, respectively. A commercial activated carbon supplied by the Carbokarn Ltd. (Thailand) under the trade name of HR5 was also used for the experiment. It was produced from coconut shell by steam activation and was designated in this work as CAC. The carbon samples were characterized for the structural porous properties by using the nitrogen adsorption isotherms at 77 K. This measurement was carried out by using an accelerated surface area and porosimetry analyzer (ASAP2010, Micromeritics, USA). The BET surface area and total pore volume were calculated from the nitrogen adsorption isotherms. Pore size distribution of carbons was also determined by the application of the density functional theory (DFT) [16] to the isotherm data. This obtained pore size distribution also gave the data of micropore volume which were calculated from the cumulative volume of the pores for pore sizes smaller than 20 Å. The combined volume of meso- and macropores was derived by subtracting the micropore volume from the total pore volume.

These selected four activated carbons were further characterized for the surface functional groups by using the Boehm titration method [17]. In this analysis, the total of the acidic and basic groups of surface functionality was determined. The analysis commenced by loading about 0.5 g of carbon samples into each of the 100 cc of 0.1 N solutions of HCl and NaOH, respectively. These mixtures were shaken for 24 h and thereafter the activated carbon suspensions were filtered. The remaining solutions were titrated with standard 0.1 N NaOH and 0.1 N HCl to determine the excess of acid and base remaining in the respective solution. The amount of acidic and basic neutralized by NaOH and HCl was then calculated and taken as the total concentration of acid and basic surface functional groups, respectively.

2. Water Adsorption Experiment

The water vapor adsorption tests were performed by using an intelligent gravimetric analyzer (IGA) supplied by Hiden Analytical Ltd., UK. This apparatus allows the measurement of adsorption and desorption isotherms of vapor or gas sorbates via the gravimetric system. Initially, the sample weighing about 0.2 g was outgassed at 300 °C for 10 h. The numbers of pressure points were specified and the adsorbed amount at equilibrium was measured for each scan of adsorption and desorption. Water adsorption isotherms for all samples were conducted at four different temperatures of 20, 25, 30 and 35 °C.

RESULTS AND DISCUSSIONS

1. Porous Characteristics of Activated Carbons

Fig. 1 shows the nitrogen adsorption isotherms of the test acti-

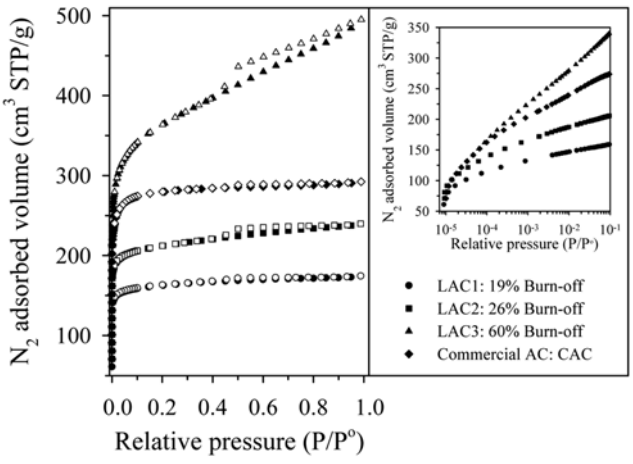

Fig. 1. Typical nitrogen adsorption isotherms at 77 K of test activated carbons; solid symbols denote adsorption, open symbols denote desorption.

Table 1. Porous properties of tested activated carbons

Sample	Burn-off (%)	BET surface area (m^2/g)	Micropore volume (cc/g)	Meso- and macropores volume (cc/g)	Total pore volume (cc/g)
LAC1	19	538	0.20 (74%)	0.07 (26%)	0.27
LAC2	26	705	0.26 (70%)	0.11 (30%)	0.37
LAC3	60	1204	0.41 (54%)	0.35 (46%)	0.76
CAC	NA	923	0.37 (82%)	0.08 (18%)	0.45

vated carbons. It is observed that the longan seed carbon series with low burn-off (<26%) as well as the commercial carbon show type I adsorption isotherm. However, at the highest burn-off of 60%, type IV isotherm is observed. The type I isotherm indicates that the activated carbons are dominated by microporosity and an increase in the size of the hysteresis loop with increased char burn-off is indicative of an increase in the proportion of mesopore volume. The small figure at the right-hand side is shown for clearer observation of the isotherms in low pressure range.

The porous properties of test activated carbons such as BET surface area, micropore volume and total pore volume were calculated from nitrogen adsorption isotherms at 77 K and are shown in Table 1. For the longan seed activated carbons, it is observed that the values of these porous properties increase with increasing in the burn-off level as expected. However, the percent of micropore volume decreases with increasing burn-off (74 to 54%). This means that the mesopore and macropore volumes increase with an increase in the degree of burn-off at the expense of micropores. It is also interesting to observe that the commercial activated carbon is highly microporous, containing about 82% of micropore volume.

Fig. 2 shows the pore size distributions (PSD) of activated carbon samples derived by using the density functional theory (DFT) (supplied by Micrometrics as DFT Plus software). This method assumes a slit-like pore geometry with the pore width being defined by the distance between the centers of carbon atoms of the two parallel graphitic layers. It is noted that there are two main peaks of PSD at pore width of 7.3 Å and 11.8 Å which are within the micropore limit (less than 20 Å). It is also seen that all the activated carbon samples contain most pores of less than 100 Å in width. The PSD curves also show that the micropore and mesopore volume (area under the curves) of longan seed activated carbon series increase with the increasing in the burn-off level.

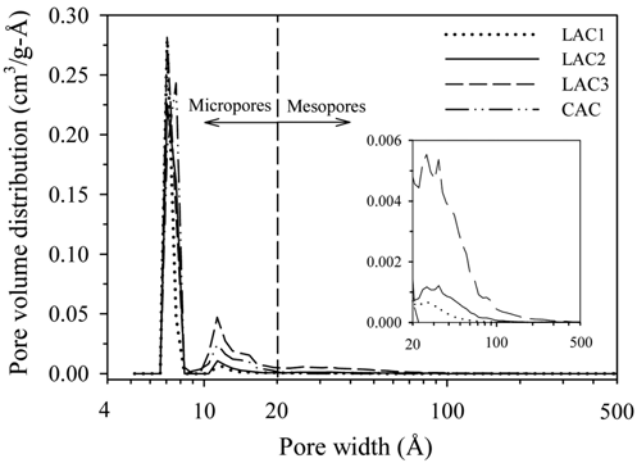

Fig. 2. Pore size distribution of activated carbons derived from DFT model

The volume-surface average pore width calculated from the DFT discrete data of pore volume are listed in Table 2. For the range of pore width less than 10 Å and between 10 to 20 Å, the average pore width for all carbon samples is approximately equal. In the mesopore size range of 20 to 500 Å, the average pore width of the LACs series increase with an increase in burn-off level in a narrow range (38.1-44.6 Å). The relatively constant pore width observed in micropores for each carbon with burn-off less than 60% agrees qualitatively with the simulation results of the carbon activation model recently proposed by Junpirom et al. [18]. They found that the basic mechanism of pore development in this regime is by the increase in the length of each pore due to the consumption of graphitic carbon layers, resulting in larger pore volume and surface area but with the average pore size remaining fairly constant. The CAC sample also contains micropores with comparable average pore width but gave much larger mesopore size.

The surface chemistry properties were also determined for the total amount of acidic and basic groups by Boehm titration as previously outlined and the results are shown in Table 3. It is seen that the amounts of surface functional groups of LACs increase with an increase in the burn-off level. The amount of surface functional group of CAC lies between those of LAC1 and LAC2. All samples were

Table 2. The average pore width in each pore size range from DFT calculation

Sample	Average pore width (Å)		
	Pore width≤10 Å	10 Å<Pore width≤20 Å	20 Å<Pore width≤500 Å
LAC1	7.4	13.5	38.1
LAC2	7.6	13.4	43.9
LAC3	7.6	13.5	44.6
CAC	7.8	13.6	92.6

Table 3. Surface chemistry property obtained from Boehm titration

Sample	Acidic (mmol/g)	Basic (mmol/g)	Total (mmol/g)
LAC1	1.00	0.92	1.92
LAC2	1.97	1.30	3.27
LAC3	2.08	1.71	3.79
CAC	1.51	1.30	2.81

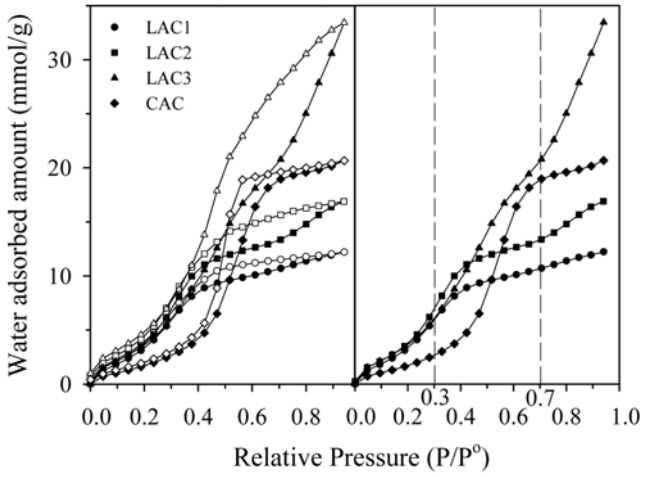

Fig. 3. Typical water adsorption isotherms at 30 °C for different activated carbons; (a) adsorption-desorption branches, (b) adsorption branch (lines are eye guides).

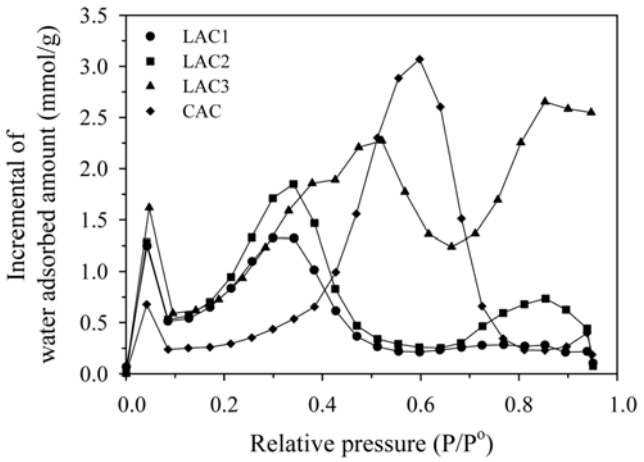

Fig. 4. The incremental of water adsorbed amount versus relative pressure (lines are eye guides).

prepared by physical activation, and these surface functional groups were introduced during the preparation step by the forming of the heteroatoms bonded with the basal plane of the aromatic sheets [19]. The increasing of surface functional groups with increasing burn-off can be possibly explained by the consequent increase of available surface area and porosity of the prepared carbons.

2. Water Adsorption Behavior

Typical water adsorption isotherms for all carbon samples at 30 °C are presented in Fig. 3 which can be approximated by type V isotherm. It is obvious that the shapes of water isotherms are different from those of the nitrogen isotherms and all of them show significant hysteresis. The size of the hysteresis loop of the LACs carbon increases with an increase in the char burn-off. This trend agrees with that of the pore width in that the average pore width in the mesopore range also increases with increasing burn-off level (see Table 2). Thus, it is inferred that the size of the hysteresis loop correlates directly with the average pore width of the large pores. This result is also in accord with the work of Miyawaki and coworkers [20] for the case of activated carbon fibers (ACF) series. It is also observed that the hystereses do not close the loops until they reach a relatively low pressure. This may arise from the difficulty in breaking the hydrogen bonds which give strong adsorption between water molecules and the functional groups on the carbon surface. These hystereses of water isotherms were reported to result from the difference between the steps involved in pore filling and pore emptying. The pore emptying involves the removal of adsorbed molecules that formed a stable phase in pores, which would be a more liquid-like phase in the central layer as the pore width is increased. Therefore, a desorption process in large pores is difficult to remove from the adsorbed phase [21].

Considering the difference in the shape of isotherms displayed by each activated carbon seems to suggest that the underlying adsorption mechanisms could be different. This postulation can be partly examined from Fig. 4 which shows plots of the incremental of water adsorbed amount versus the relative pressure. All carbons show roughly three main peaks of curves. For relative pressures lower than 0.7, the curves give a narrow initial peak exhibited by all carbon samples, followed by the main peak at 0.3 for LAC1 and LAC2, 0.5 for LAC3 and 0.6 for CAC, respectively. At higher relative pressures, LAC2 and LAC3 show a significant peak at the relative pressure of 0.85. It is seen that different carbon samples show similar pattern of changes except the differences in the peak position. Therefore, it could be hypothesized that the mechanisms involved in water adsorption by the various carbons with respect to pressure change may be fundamentally the same. With reference to this adsorption behavior and the shapes of the isotherm curves in Fig. 3, it might be reasonable to divide the adsorption into three ranges of relative pressure, namely 0.0-0.3, 0.3-0.7 and 0.7-0.94, as illustrated in Fig. 3(b).

At the low relative pressure of 0.0-0.3, the adsorbed amount increased continuously with increasing pressure. The adsorbed amounts of the LACs are relatively the same and greater than that of the CAC. In the range of relative pressure from 0.3-0.7, the steep increasing of the amount adsorbed occurs for the LAC3 and CAC, while the LAC1 and LAC2 still show an increase but with a much lesser extent. The LAC3 continue to show a further sharp increase in the adsorbed amount for relative pressure greater than 0.7, while the rest of LAC series give marginal increasing with LAC2 showing a slight inflection at the relative pressure of 0.7. The CAC shows similar behavior to LAC1 and LAC2 in the last pressure range but with higher adsorption capacity.

Table 4 shows the micropore volume derived from the DFT calculation and the pore volume computed from water adsorption iso-

Table 4. Pore volume derived from the DFT analysis of N_2 (77 K) data and the adsorbed water amount

Sample	Micropore volume from DFT (V^{DFT}) (cc/g)	Pore volume estimated from adsorbed water (V^{H2O}) (cc/g)
	Pore width≤20 Å	$0.0 \le P/P^o \ge 0.7$
LAC1	0.202	0.209
LAC2	0.264	0.262
LAC3	0.410	0.407
CAC	0.370	0.371

therms estimated up to the relative pressure of 0.7. It is observed that these two values are surprisingly agreeable. This indicates that the water adsorption mechanism for the relative pressure up to 0.7 should involve the adsorption in micropores. This number is comparable to that reported by Alcaniz-Monge and coworkers [22,23] who found the water adsorption up to the relative pressure of about 0.8 to result from micropore filling. It is also interesting to observe the adsorption behavior in the low pressure range up to around 0.3, as appears in Fig. 3. The water uptake is quite different between the LACs series and the CAC, with the latter giving a lesser adsorbed amount. This difference could be ascribed to the difference in characteristics of porous structure, surface structure and surface functional group properties of each type of carbon material. In addition, the similarity of water isotherms in this low pressure range for the LACs series deserves further examination. The information in Table 5 shows the values of the ultramicropore volume (pore width less than 7 Å) and the corresponding relative pressure of the water isotherms that the water accessed this volume. From these results, it can be said that the calculated relative pressures of the LACs series in Table 5 are comparable and close to the value of 0.3 at which their isotherms start to separate from each other (see Fig. 3). This indicates that at the relative pressure less than 0.3 the water adsorption is controlled to a greater extent by the adsorption in ultramicropores. For relative pressures higher than 0.7, water uptake increases with increasing char burn-off, mainly due to the corresponding increase of the mesopore and macropore volume. It can thus be inferred that pore size distribution of activated carbon plays a significant role in the adsorption behavior of water inside the pores with water being adsorbed in all sizes of pores with respect to the pressure change. It is generally accepted that water adsorption in activated carbon involves the adsorption of the first water molecule onto acidic surface groups followed by further adsorption via hydrogen bonding between water molecules [4-6]. Therefore, the effect of pore size distribution on water adsorption behavior of the non-oxidized activated carbon could be viewed as the role and effect of surface functional groups which distribute in various pore sizes.

Fig. 5 shows additional isotherm data for water adsorption at various temperatures including 20, 25, 30 and 35 °C. Regarding the adsorption isotherms that are plotted versus pressure, it is clear that the water uptake decreases when the adsorption temperature is increased, indicating that water adsorption involves the liberation of heat. It is also interesting to observe that the temperature has no distinct effect on the shape of water isotherms in that all the isotherm

Table 5. Estimated relative pressure from water isotherms for volume adsorbed corresponding to ultramicropore volume

Sample	V^{DFT} (cc/g) (Pore width≤7.33 Å)	P/P^o of H_2O isotherms [$V^{H2O}=V^{DFT}$ (Pore width≤7.33 Å)]
LAC1	0.150	0.361
LAC2	0.122	0.289
LAC3	0.152	0.347
CAC	0.101	0.433

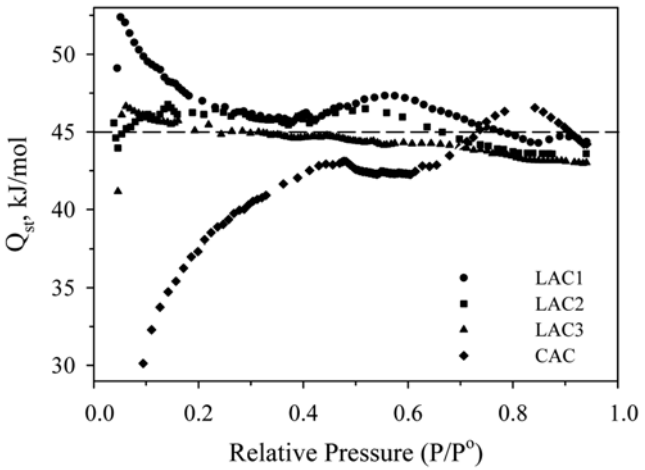

Fig. 6. Isosteric heat of water adsorption for different activated carbons.

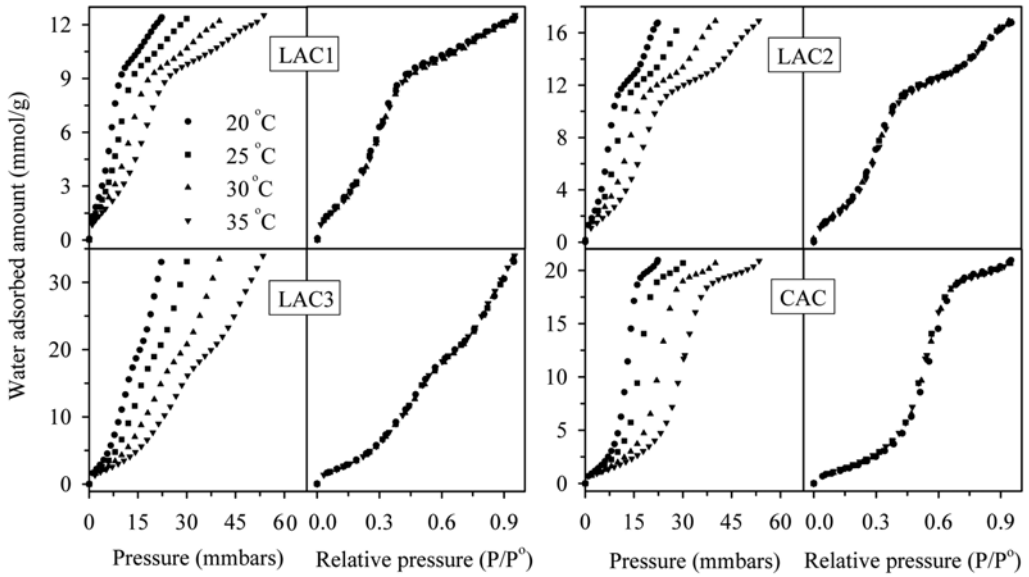

Fig. 5. Water adsorption isotherms for different activated carbons at various temperatures.

curves fall into one single curve when the isotherm is plotted against the relative pressure, as shown in Fig. 5. The isosteric heat of adsorption (Q_{st}) was calculated from these isotherms data by employing the van't Hoff equation [24], giving results as shown in Fig. 6. The Q_{st} of LACs appear to vary, over almost the entire range of relative pressure, in the vicinity of 45 kJ/mol, which is the latent heat of bulk water condensation [6,7]. However, a different trend occurs for the CAC such that the Q_{st} increases first with pressure and reaches a maximum around 42.9 kJ/mol at a relative pressure of 0.5 before approaching the value closer to 45 kJ/mol at relative pressures higher than 0.7.

3. Simulation of Water Adsorption Isotherms

Since the DS equation has been widely used for describing water adsorption isotherms, it was first adopted to check the model validity. The model equation is presented as Eq. (1) and can be arranged to obtain the explicit form of adsorbed-phase concentration as shown in Eq. (2):

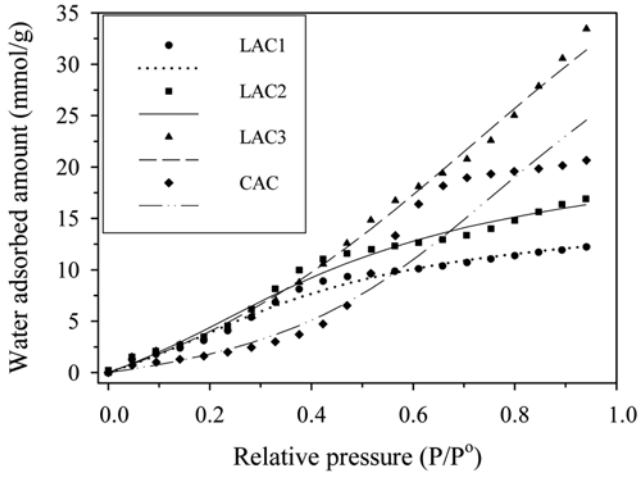

Fig. 7. Fitting of the Dubinin-Serpinsky model (DS) to the experimental water isotherms of activated carbon series: symbols denote experimental data, lines denote fitted results.

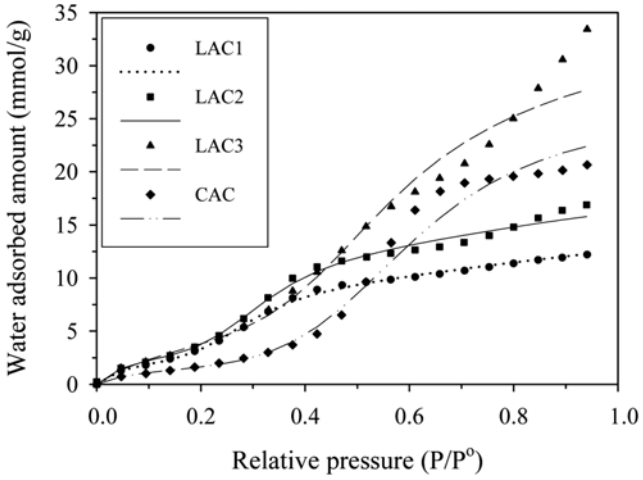

Fig. 8. Fitting of the original Do and Do model to the experimental water isotherms carbon series; symbols denote experimental data, lines denote fitted result.

$$x = \frac{C_\mu}{c(1-kC_\mu)(C_{\mu 0}+C_\mu)} \tag{1}$$

$$C_\mu = \frac{-\frac{1}{k}\left(\frac{1}{cx}+kC_{\mu 0}-1\right)+\sqrt{\frac{1}{k^2}\left(\frac{1}{cx}+kC_{\mu 0}-1\right)^2+\frac{4C_{\mu 0}}{k}}}{2} \tag{2}$$

where x is relative pressure (P/P^o), C_μ is the adsorbed water concentration, $C_{\mu 0}$ is the concentration of the primary sites, k represents the loss of the secondary sites due to the finiteness of the adsorbed volume, and c is the ratio of the rate constants.

The fitted results to the isotherm data by DS equation are displayed in Fig. 8. The results show that the DS model can describe the CAC isotherm reasonably correctly up to the relative pressure of about 0.45 but fails completely at higher relative pressure values. For the LAC series, the DS model can fit the lowest burn-off carbon (LAC1) well except over the intermediate pressure range (relative pressure: 0.35-0.50) where the model underpredicts the experimental data. For higher burn-off samples (LAC2 and LAC3), the model can predict the correct trend of isotherm data but cannot account for the inflection characteristics of the isotherm curves.

Recently, Do and Do [7] have proposed another model for water adsorption in activated carbon. The development of this model was based on the growth of a cluster of water molecules around the surface functional groups to form a pentamer cluster and followed by the adsorption of this cluster into the micropores. This model is able to describe most water adsorption behaviors of non-polar surface carbon as well as highly oxidized carbon. The final model equation reads

$$C_\mu = S_0\frac{K_f\sum_{n=1} nx^n}{1+K_f\sum_{n=1} x^n} + C_{\mu s}\frac{K_\mu\sum_{n=6} x^n}{K_\mu\sum_{n=6} x^n+\sum_{n=6} x^{n-5}} \tag{3}$$

where C_μ is the water vapor adsorbed amount, x is the relative pressure, S_0 is the functional group concentration, K_f is the chemisorption equilibrium constant, $C_{\mu s}$ is the saturation concentration of water in micropore, K_μ is the micropore equilibrium constant, and n is the number of water molecules in a cluster usually taken as five.

This model was tested against the experimental data and the results are shown in Fig. 8, and Table 6 shows the model parameters obtained from the data fitting. It is seen that the model can describe only the data of LAC1 carbon very well over the entire range of relative pressure. However, the isotherms of other carbons can be fitted with reasonable accuracy more or less up to the relative pressure around 0.5. The mismatch of the simulated results with experimental isotherms at higher pressures, corresponding to adsorption

Table 6. The optimized parameters derived from the water adsorption model of Do and Do

Sample	Simulated parameter					
	S_0 (mmol/g)	K_f	$C_{\mu s}$ (mmol/g)	K_μ	n	r^2
LAC1 (19%)	2.38	20.84	5.49	504.5	5	0.998
LAC2 (26%)	2.93	18.69	7.49	316.8	5	0.992
LAC3 (60%)	4.36	8.28	16.45	22.7	5	0.971
CAC	1.54	15.30	19.85	13.3	5	0.979

Table 7. The optimized parameters derived from the modified isotherm model of Do and Do

Sample	Relative pressure	Simulated parameter				
		S_0 (mmol/g)	K_f	$C_{\mu s}$ (mmol/g)	K_μ	n
LAC1	($0.0<P/P^o\leq0.94$)	2.38	20.84	5.49	504.5	5
LAC2	($0.0<P/P^o\leq0.70$)	2.56	27.06	7.80	387.4	5
	($0.70<P/P^o\leq0.94$)	0.004	100.07	3.58	38.8	20
LAC3	($0.0<P/P^o\leq0.70$)	3.59	12.42	13.80	47.2	5
	($0.70<P/P^o\leq0.94$)	0.089	12.20	12.05	46.6	20
CAC	($0.0<P/P^o\leq0.66$)	2.02	8.80	19.97	42.9	7
	($0.66<P/P^o\leq0.94$)	0.614	0.013	1.06	157.5	20

in large pores, suggesting that the adsorption behavior of water should depend on the pore size. Therefore, we propose to modify this model to account for the effect of pore size on adsorption by dividing the pressure into two ranges: adsorption at low and high pressure ranges. In the low pressure range, the experimental data were fitted directly by the model equation with five water molecules in a cluster (a pentamer) while the cluster size can be changed for simulation at the high pressure range. The exact relative pressure at which the change in the cluster size occurred was determined for each activated carbon by a trial-and-error search procedure to give the best fit between the simulated and experimental isotherms.

Table 7 lists the optimum parameters derived by the modified model outlined earlier and Fig. 9 shows the calculated results. It is observed that the model can describe the data extremely well for all samples investigated in this work, except for the LAC3 sample at relative pressures greater than 0.9 where the effect of capillary condensation could occur [7]. The LAC2 and LAC3 show the inflection points at the relative pressure of 0.7 with 5 and 20 water molecules in a cluster for adsorption at relative pressures lower and higher than 0.7, respectively. The inflection point of CAC was found to be 0.66 with the cluster size being 7 and 20 for the lower and higher relative pressure range, respectively. The cluster size obtained in this work for adsorption in micropores (5 and 7) is comparable to the values of 8-10 for the optimum cluster size for adsorption in graphite nanopore (pore width 1.1 nm) as reported by Ohba et al. [15] and Kimura et al. [25].

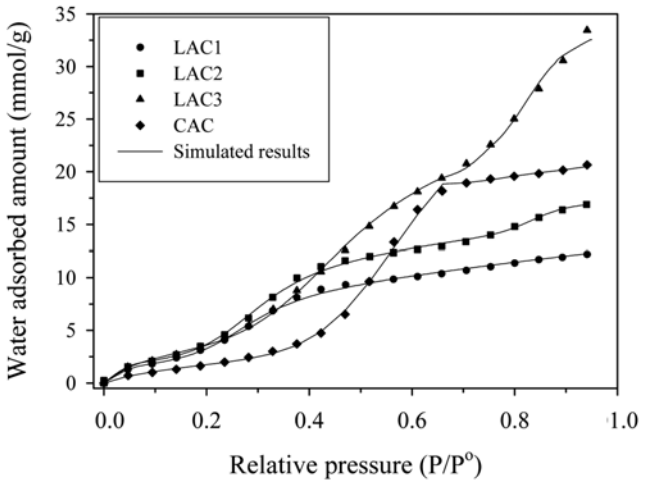

Fig. 9. Fitting of the modified isotherm model of Do and Do to the experimental water isotherms of carbon series; symbols denote experimental data, lines denote fitted results.

The model parameters shown in Table 7 reflect the chemical nature of the carbon surface. For example, S_0 and $C_{\mu s}$ are two relevant parameters which involve the surface functional group concentration and the saturation concentration in the micropore, respectively. For the LAC series the S_0 and $C_{\mu s}$ of micropores ($P/P^o<0.7$) show an increase with increasing burn-off with the values of 2.38, 2.56 and 3.59 mmol/g and of 5.49, 7.80 and 13.80 mmol/g for the burn-off of 19, 26 and 60%, respectively. For adsorption in mesopores ($P/P^o>0.7$) the S_0 and $C_{\mu s}$ of LAC2 and LAC3 also increase with increasing burn-off. These increases are consistent with the higher specific surface area and pore volume of the carbons as the burn-off is increased. It is observed that the total of S_0 and the concentration of acidic surface group from Boehm titration of the LACs carbons follows the same trend. Those S_0 are 2.38, 2.56 and 3.68 mmol/g while the Boehm's results are 1.00, 1.97 and 2.08 mmol/g, for the activated carbons LAC1, LAC2, and LAC3, respectively.

The two-step simulation scheme clearly indicates the different adsorption mechanism in the low and high pressure ranges corresponding to adsorption in micropores and meso- and macropores, respectively. At low pressures up to the relative pressure of 0.7 the adsorption involves micropore filling with the pentamer clusters of water for the LACs series and a cluster of 7 molecules for the coconut shell-based activated carbon. The difference in cluster size between these two raw materials is possibly ascribed to the differences in porous structure and surface functionalities of each carbon sample. For the relative pressures greater than 0.7 the adsorption occurs in the mesopores and macropores with the increase in cluster size. The increased cluster size in mesopore adsorption is the result of the lower interaction energy of solid surface and adsorbate molecules in mesopores as compared to that in micropores.

CONCLUSIONS

Activated carbons with different pore size distribution were produced by controlling the burn-off level during carbon dioxide activation of longan seed char. The variation of char burn-off also affected the concentration of surface functional groups of the activated carbons. The resultant carbons were used to study the effect of combined influences of pore structure and surface properties on water adsorption behavior. The results obtained from this work showed that the water adsorption isotherm depended significantly on the pore size distribution through the role of acidic surface functional

groups. It was found that water can adsorb into all pore sizes including, ultramicropores, supermicropores and larger pores (mesopores and macropores), corresponding to adsorption in the following range of relative pressure, 0.0-0.3, 0.3-0.7 and 0.7-0.94, respectively. The heat of adsorption calculated from the isotherms for activated carbon with different burn-offs had values comparable to the latent heat of water condensation of 45 kJ/mol, indicating the significance of water molecular interaction. Modification of the water isotherm model of Do and Do by considering the adsorption in micropore and larger pores with different cluster sizes gave a full description of water adsorption in porous carbons. The cluster formation before being adsorbed into micropores and larger pores is different with regard to the size of the cluster. For adsorption in micropores the water cluster sizes are 5 and 7 molecules for the longan seed and coconut shell based carbon, respectively. The cluster size needed to be adjusted to 20 molecules for the adsorption into the meso- and macropores for both types of carbons. Further work should be directed toward studying the effects of concentration and density distribution of acidic functional groups on water adsorption. This may be achieved by the use of strong oxidizing agent, e.g., HNO_3 and by selective control of the type of acidic surface groups existing on the carbon surface by thermal treatment.

ACKNOWLEDGMENT

Financial support from the Thailand Research Fund (TRF) through the Royal Golden Jubilee Ph.D. Program (Grant No. PHD/0087/2543) is gratefully acknowledged.

NOMENCLATURE

c : ratio of the rate constant
C_μ : water adsorbed concentration [mmol/g]
$C_{\mu 0}$: concentration of the primary sites [mmol/g]
$C_{\mu s}$: saturation concentration of water adsorbed in micropore [mmol/g]
k : represents the loss of the secondary sites due to the finiteness of adsorbed volume [$(mmol/g)^{-1}$]
K_f : chemisorption equilibrium constant
K_μ : micropore equilibrium constant
n : number of water molecules in a cluster
P, P^o : gas phase pressure and vapor pressure, respectively [mmbar]
Q_{st} : isosteric heat of adsorption [kJ/mol]
S_0 : functional group concentration [mmol/g]
x : relative pressure (P/P^o)

REFERENCES

1. S. Y. Cho, S. S. Park, S. J. Kim and T. Y. Kim, *Korean J. Chem. Eng.*, **23**, 638 (2006).
2. M. G. Lee, S. W. Lee and S. H. Lee, *Korean J. Chem. Eng.*, **23**, 773 (2006).
3. B. H. Kim, G. H. Kum and Y. G. Seo, *Korean J. Chem. Eng.*, **20**, 104 (2003).
4. N. J. Foley, K. M. Thomas, P. L. Forshaw, D. Stanton and P. R. Norman, *Langmuir*, **13**, 2083 (1997).
5. D. D. Do and H. D. Do, *Carbon*, **38**, 767 (2000).
6. J. K. Brennan, T. J. Bandosz, K. T. Thomson and K. E. Gubbins, *Colloids Surf. A*, **187-188**, 539 (2001).
7. I. I. Salame and T. J. Bandosz, *Langmuir*, **15**, 587 (1999).
8. M. M. Dubinin and V. V. Serpinsky, *Carbon*, **19**, 402 (1981).
9. E. A. Müller, L. F. Rull, L. F. Vega and K. E. Gubbins, *J. Phys. Chem.*, **100**, 1189 (1996).
10. E. A. Müller and K. E. Gubbins, *Carbon*, **36**, 1433 (1998).
11. C. L. McCallum, T. J. Bandosz, S. C. McGrother, E. A. Müller and K. E. Gubbins, *Langmuir*, **15**, 533 (1999).
12. G. R. Birkett and D. D. Do, *Mol. Phys.*, **104**, 623 (2006).
13. K. Kaneko, Y. Hanzawa, T. Iiyama, T. Kanda and T. Suzuki, *Adsorption*, **5**, 7 (1999).
14. T. Ohba, H. Kanoh and K. Kaneko, *J. Am. Chem. Soc.*, **126**, 1560 (2004a).
15. T. Ohba, H. Kanoh and K. Kaneko, *J. Phys. Chem. B*, **108**, 14964 (2004b).
16. J. P. Olivier, *J. Porous Mater.*, **2**, 9 (1995).
17. H. P. Boehm, *Carbon*, **40**, 145 (2002).
18. S. Junpirom, D. D. Do, C. Tangsathitkulchai and M. Tangsathitkulchai, *Carbon*, **43**, 1936 (2005).
19. R. C. Bansal, J. B. Donnet and F. Stoeckli, *Active carbon*, Marcel Dekker, New York (1988).
20. J. Miyawaki, T. Kanda and K. Kaneko, *Langmuir*, **17**, 664 (2001).
21. F. Rouquerol, J. Rouquerol and K. Sing, *Adsorption by powder and porous solids: Principles, methodology and applications*, Academic Press, London (1999).
22. J. Alcaniz-Monge, A. Linares-Solano and B. Rand, *J. Phys. Chem. B*, **105**, 7998 (2001).
23. J. Alcaniz-Monge, A. Linares-Solano and B. Rand, *J. Phys. Chem. B*, **106**, 3209 (2002).
24. S. J. Gregg and K. S. W. Sing, *Adsorption, surface area and porosity*, Academic Press, London (1982).
25. T. Kimura, H. Kanoh, T. Kanda, T. Ohkubo, Y. Hattori, Y. Higaonna, R. Denoyel and K. Kaneko, *J. Phys. Chem. B*, **108**, 14043 (2004).